

## Distance Matrices, Wiener Indices, and Related Invariants of Fullerenes

P. W. Fowler,<sup>\*,†</sup> G. Caporossi,<sup>‡</sup> and P. Hansen<sup>\*,§</sup>

School of Chemistry, University of Exeter, Stocker Road, Exeter, U.K. EX4 4QD, École Polytechnique de Montréal, Case Postale 6079, Centre-ville, Montréal Québec, Canada H3C 3A7, and GERAD and École des Hautes Études Commerciales de Montréal, 3000 Chemin de la Côte-Sainte-Catherine, Montréal, Québec, Canada H3T 2A7

Received: February 5, 2001

The distance matrix of a chemical graph can be computed in quadratic time and from it can be obtained the distance level patterns (DLP); Wiener, Szeged, and Balaban indices; as well as the distance eigenvalues. Point-group symmetry places bounds on the numbers of distinct DLP and distance eigenvalues. Angular-momentum arguments rationalize the distance spectrum for near-spherical cages. Wiener and Balaban indices are inversely correlated and select fullerenes from general cubic polyhedra and isolated-pentagon from general fullerenes. In combination with hexagon-neighbor information, all three named indices select low-energy isolated-pentagon fullerenes at 84 and 100 atoms.

### 1. Introduction

Perhaps the most natural description of a molecular graph is in terms of the distances, geometric or topological, between its pairs of vertices. Distance-based invariants have a long history in chemistry and have found useful application in structure–property correlations. The oldest topological invariant is the Wiener index, which was proposed over half a century ago<sup>1</sup> as a measure of compactness of acyclic alkanes correlating with boiling points and other thermochemical properties. Many variants have since been devised, some including generalized distances and volumes for chemical graphs<sup>2</sup> and applications of the Wiener index itself have been proposed for ever wider classes of molecules.<sup>3</sup> Wiener indices have been calculated for a number of fullerene isomers,<sup>4–6</sup> and for some systematic sets,<sup>7</sup> but correlation with energetic or other properties of these already compact pseudospherical molecules does not seem to have been reported.

It has been suggested that more of the information that is contained in the full distance matrix **D** could be used with advantage in the study of fullerenes. (**D** is the matrix with elements  $D_{ij}$  the number of edges in the shortest walk along edges from  $i$  to  $j$ ). For example, Balasubramanian<sup>5,6</sup> obtains a *distance level pattern* and a corresponding *distance level diagram* by ordering the entries of one column of **D** and then the *distance spectrum* and its *distance characteristic polynomial* by diagonalizing **D**. Various features of distance spectra of fullerenes are noted in passing. The level pattern itself is also advanced in those papers as a candidate for a discriminatory structural invariant of fullerenes, though as will be shown below, this cannot be correct, because the details of the pattern depend on the choice of root vertex. It seems desirable to evaluate the various literature proposals by making a systematic survey that uses an efficient algorithm, includes rigorous consideration of the symmetry properties of **D** and takes advantage of the

considerable body of data on fullerene energetics that is already available.

The current paper has therefore the following aims: (a) to correct some erroneous literature claims for distance-level patterns of fullerenes and to explore the distance spectrum as a mathematically well defined alternative; (b) to present an efficient algorithm for computation of the distance matrix **D** and related invariants and to apply it to fullerenes and other cubic polyhedra; and (c) to investigate the ability of Wiener and related indices to distinguish fullerenes from general cubic polyhedra, isolated-pentagon fullerenes from general fullerenes, and stable from unstable fullerenes.

The outline of the paper is as follows. After a summary of basic definitions (section 2), the correct relationship between Wiener index and distance level patterns is stated (section 3) and general features of the distance spectra of polyhedra are analyzed using symmetry arguments and an analogy with simpler systems (section 4). A brief discussion of efficient algorithms (section 5) is followed by a report of explicit calculations on fullerenes and other trivalent polyhedra (section 6).

### 2. Definitions

The distance matrix **D** is defined as follows: if  $i = j$ , then

$$D_{ij} = 0 \quad (1)$$

but if  $i \neq j$

$$D_{ij} = d_{ij} \quad (2)$$

where  $d_{ij}$  is the length of the shortest walk from  $i$  to  $j$ . A walk is defined here as a sequence of consecutive edges starting from the vertex  $i$  and terminating at vertex  $j$ , and its length is measured by the number of edges traversed, without considering their geometric lengths. The adjacency matrix **A** of the graph is then

$$A_{ij} = 1 \quad (3)$$

\* To whom correspondence should be addressed.

† University of Exeter.

‡ École Polytechnique de Montréal.

§ GERAD and École des Hautes Études Commerciales de Montréal.

if and only if  $d_{ij} = 1$ , and otherwise

$$A_{ij} = 0 \quad (4)$$

The Wiener index  $W$  is

$$W = \frac{1}{2} \sum_{i=1}^n \sum_{j=1}^n d_{ij} = \sum_{i>j=1}^n d_{ij} \quad (5)$$

i.e., the sum of shortest pairwise distances taken over all distinct pairs of vertices. The average distance between noncoincident vertices in the graph is  $\bar{d}$  and is recovered from  $W$  as

$$\bar{d} = \frac{2W}{n(n-1)} \quad (6)$$

A related quantity is the Szeged index introduced by Gutman,<sup>8</sup> which has contributions from all edges of the graph:

$$Sz = \sum_{\text{edges}} n_i n_j \quad (7)$$

where, for any edge  $ij$ ,  $n_i$  counts the vertices of  $G$  that are closer to vertex  $i$  than to  $j$  and  $n_j$  counts those that are closer to  $j$  than to  $i$ , with vertices equidistant from  $i$  and  $j$  being ignored. This is a natural generalization of the Wiener index, because (7) is actually the formula used by Wiener to evaluate  $W$  for trees<sup>1</sup> (for which  $W = Sz$ ), and the two indices correlate for various derivative classes of graph.<sup>9</sup> For cubic graphs, the naive asymptotic upper bound on  $Sz$  is  $\sim 3n^3/8$ , achieved if all  $3n/2$  edges simultaneously have the maximal  $n_i = n_j = n/2$  (as in the  $2n$ -gonal prism but not, e.g., in a polyhedron with one or more odd faces).

A third invariant defined from the distance matrix is the Balaban index  $J$ <sup>10</sup>

$$J = \frac{b}{c+1} \sum_{\text{edges}} (d_i d_j)^{-1/2} \quad (8)$$

where  $b$  is the number of edges,  $c$  is the number of primitive cycles ( $b = 3n/2$  and  $c + 1 = n/2 + 2$  for a cubic graph), and  $d_i$  is the row sum

$$d_i = \sum_{j=1}^n d_{ij} \quad (9)$$

For the specific *polyhedral* graphs in which all vertices have the same row sum (e.g., the Platonic and Archimedean solids), a simple relationship connects the Balaban and Wiener indices via the numbers of faces, edges, and vertices,  $f$ ,  $e$ ,  $v$ :

$$WJ = \frac{1}{2} v e^2 / f \quad (10)$$

(If the polyhedron is cubic, the RHS of (10) is  $9v^3/4(v+4)$ ). Balasubramanian<sup>5</sup> notes the analogy between  $J$  and the Randić connectivity index<sup>11</sup>

$$\chi = \sum_{\text{edges}} (v_i v_j)^{-1/2} \quad (11)$$

where

$$v_i = \sum_{j=1}^n A_{ij} \quad (12)$$

is the degree of the vertex  $i$ . For any regular graph,  $\chi$  is trivially  $n/2$ .

The radius  $R$  and diameter  $D$  of a graph are also readily calculated from  $\mathbf{D}$ . If the *eccentricity* of a vertex  $i$  is defined as the largest entry in the row  $\{d_{ij}\}$ , the *center* of the graph is then the set of vertices of minimal eccentricity, and the *radius* is the eccentricity of these central vertices. The *diameter* is the largest eccentricity of any vertex and obeys  $D \leq 2R$ . Some conjectured relations between  $D$ ,  $R$ , and other invariants for fullerenes are given by the GRAFFITI program<sup>12,13</sup> and are subjected to computational test in ref 14. The recently proposed<sup>15</sup> "reverse Wiener index" combines diameter and  $W$  and is equal to  $n(n-1)D/2 - W$ .

### 3. Distance Level Patterns

For a given vertex  $i$  in a fullerene or other cubic polyhedron, it is possible to define the *distance level pattern* as the ordered sequence of values  $d_{ij}$  running through consecutive integers up to the eccentricity of vertex  $i$ . This distance level pattern is also known in mathematical graph theory<sup>16</sup> as the *level representation* of the graph  $G$  with respect to the vertex  $i$ . More compactly, the pattern is given as the list of the multiplicities  $g_k$  of distance  $k$ . Thus, a vertex of the dodecahedral  $C_{20}$  fullerene has three neighbors at distance 1, six at distance 2, six at 3, three at 4, and one (the antipodal vertex) at distance 5; in the notation of ref 6, the distance level pattern for the vertex is therefore 0(1), 1(3), 2(6), 3(6), 4(3), and 5(1), or simply  $\{1, 3, 6, 6, 3, 1\}$ . Note that, unusually among fullerenes, this sequence for  $C_{20}$  is palindromic. [An infinite set of graphs for which every DLP is palindromic is that of the  $d$ -dimensional hypercubes  $\gamma_d$ . Each  $\gamma_d$  has diameter  $d$  and DLP equal to the  $(d+1)$ th row of the Pascal triangle,  $\{1\}$  for  $d=0$ ,  $\{1, 1\}$  for  $d=1$ ,  $\{1, 2, 1\}$  for  $d=2$ , etc.]

However, in contradiction to statements in at least two published sources,<sup>5,6</sup> the distance level pattern is *not* invariant to the choice of  $i$  in general fullerenes. Indeed, an assumption of invariance would fail at only the second fullerene,  $C_{24}$ , which already has two distinct level patterns (Figure 1). Among isolated-pentagon fullerenes, the assumption would also fail at the second instance;  $C_{70}$  has five distinct distance level patterns of two different lengths:  $\{1, 3, 6, 8, 10, 11, 11, 10, 7, 3\}$ ,  $\{1, 3, 6, 8, 11, 11, 11, 10, 6, 3\}$ ,  $\{1, 3, 6, 8, 10, 10, 10, 9, 7, 4, 2\}$ ,  $\{1, 3, 6, 8, 10, 10, 11, 9, 6, 6\}$ , and  $\{1, 3, 6, 9, 10, 11, 12, 9, 6, 3\}$ , where the first two are each realized by 20 and the last three by 10 vertices. Only the polar vertices have distances equal to the full diameter of the graph ( $D = 10$ ).

Vertices of a polyhedron fall into *orbits*, i.e., sets of equivalent points such that symmetry operations permute vertices within but not between sets, and for a given polyhedron, the distance level patterns are equal for symmetry-equivalent vertices but not necessarily for vertices belonging to different orbits. Only  $C_{20}$  and  $I_h C_{60}$  are one-orbit fullerenes and are, thus, the *only* two fullerenes guaranteed by symmetry to have vertex-invariant distance level patterns. In the language of graph theory,  $C_{20}$  and  $C_{60}$  are both vertex-transitive.  $C_{20}$  is also, uniquely among the fullerenes, edge-transitive.

Although the DLP for an individual vertex is not a graph invariant, invariants based on the whole sets of level patterns can of course be constructed. The simplest such combination



in the orbit formulation are

$$d(G, 0) = \sum_k n_k$$

$$d(G, l \geq 1) = \frac{1}{2} \sum_k n_k g_{k,l}$$

and it has the properties  $d(G, 0) = n$ ,  $d(G, 1) = m$ ,  $(dH(G, x)/dx)_{x=1} = \sum_{l \geq 0} ld(G, l) = W(G)$ ,  $H(G, 1) = n(n+1)/2$  for an  $n$ -vertex,  $m$ -edge graph. Hosoya polynomials for the fullerenes featured in Table 1 are straightforwardly recovered from the data listed there. For the two single-orbit fullerenes

$$H(C_{20}, x) = 20 + 30x + 60x^2 + 60x^3 + 30x^4 + 10x^5$$

$$H(C_{60}, x) = 60 + 90x + 180x^2 + 240x^3 + 300x^4 + 300x^5 + 300x^6 + 240x^7 + 90x^8 + 30x^9$$

#### 4. Distance Spectra

The distance matrix  $\mathbf{D}$  can be diagonalized, and as a real symmetric  $n \times n$  matrix, it has  $n$  real eigenvalues  $\{\lambda^D\}$ . The symmetry spanned by the eigenvectors of  $\mathbf{D}$  is  $\Gamma_\sigma(v)$ , the permutation representation of the vertices in the maximal point group of the fullerene. It is identical to the symmetry spanned by the eigenvectors of the adjacency matrix, which correspond to eigenvalues  $\{\lambda^A\}$ . Multiplication by the representation of a local basis function (which for a polyhedron with "radial"  $\pi$  orbitals is  $\Gamma_0$ , the totally symmetric representation) gives the representation of the Hückel molecular orbitals (i.e., the linear combinations of basis functions that diagonalize the Hamiltonian matrix  $\alpha\mathbf{I} + \beta\mathbf{A}$  where  $\alpha$  and  $\beta$  are constants<sup>19</sup>).

The two matrices  $\mathbf{A}$  and  $\mathbf{D}$  carry exactly the same information content, because  $\mathbf{D}$  can be computed from the powers of  $\mathbf{A}$  and the nonzero components of  $\mathbf{A}$  are simply the set of unit entries in  $\mathbf{D}$ .<sup>20</sup> However, it can be anticipated that the information content/discriminatory power of the spectrum  $\{\lambda^D\}$  will be smaller than that of  $\{\lambda^A\}$  because many distance spectra have very high "accidental" degeneracies of the zero eigenvalue. Balasubramanian has calculated characteristic polynomials and numerical eigenvalues of  $D$  for a sample set of fullerenes.<sup>5,6</sup>

The permutation representation of the vertices carries symmetry information on both  $W$  and  $\mathbf{D}$ . In its reduced form,  $\Gamma_\sigma(v)$  is a linear combination of the irreducible representations  $\Gamma_i$  of the relevant group:

$$\Gamma_\sigma(v) = \sum_i a_i \Gamma_i \quad (14)$$

In this expansion,  $a_0$  (the coefficient of  $\Gamma_0$ ) is equal to the number of distinct orbits of vertices. The symmetric square  $[\Gamma_\sigma(v)^2]$  gives the representation of all possible distinct pairings of vertices (including pairings of a vertex with itself). Subtraction of the zero-length walks gives  $[\Gamma_\sigma(v)^2] - \Gamma_\sigma(v)$ , and the number of copies of  $\Gamma_0$  in this representation is therefore

$$\sum_i \frac{1}{2} a_i (a_i + 1) - a_0 \quad (15)$$

which is equal to the number of orbits of symmetry-distinct vertex pairs in the graph. The number of numerically distinct entries in  $\mathbf{D}$  may of course be smaller, as pairs that are not

equivalent by symmetry may still have equal separation, and thus

$$\sum_i \frac{1}{2} a_i (a_i + 1) - a_0 \geq D \quad (16)$$

The equality is realized by *distance transitive* graphs. A distance transitive graph is one in which  $d_{ij} = d_{uv}$  implies that the vertex pairs  $(i, j)$  and  $(u, v)$  are equivalent by symmetry. Such graphs have  $D + 1$  distinct adjacency eigenvalues  $\lambda_A$ .<sup>21</sup>  $C_{20}$  is an example which illustrates the fact that distance-transitive graphs do not necessarily have  $D + 1$  distinct *distance* eigenvalues  $\lambda_D$ .

If  $\Gamma_\sigma(v)$  has a block with  $a_i = 1$ , the eigenvectors of  $\mathbf{D}$  of that symmetry are fully determined and, hence, coincide with those of  $\mathbf{A}$  in the same symmetry block for the graph in question. For fullerenes without symmetry, (16) reduces to the loose bound

$$\frac{1}{2} n(n-1) \geq D \quad (17)$$

As concrete examples, consider the dodecahedral  $C_{20}$  and truncated icosahedral  $C_{60}$  fullerenes, both of  $I_h$  symmetry. For  $C_{20}$ , the vertex representation is

$$\Gamma_\sigma(20) = A_g + G_g + H_g + T_{1u} + T_{2u} + G_u \quad (18)$$

and

$$[\Gamma_\sigma(20)^2] - \Gamma_\sigma(20) = 5A_g + 2T_{1g} + 2T_{2g} + 7G_g + 11H_g + A_u + 5T_{1u} + 5T_{2u} + 6G_u + 7H_u \quad (19)$$

implying that all vertices belong to a single orbit but that the 190 shortest walks of nonzero length fall into 5 distinct sets, one for each length  $l = 1-5$ . All eigenvectors of  $\mathbf{A}$  for  $C_{20}$  are therefore also eigenvectors of  $\mathbf{D}$ . The separate orbits of vertex pairs span representations reflecting the site groups  $C_{2v}$ ,  $C_s$ ,  $C_2$ ,

$$\Gamma(l=1) = A_g + G_g + 2H_g + T_{1u} + T_{2u} + G_u + H_u \quad (20)$$

$$\Gamma(l=2) = A_g + T_{1g} + T_{2g} + 2G_g + 3H_g + 2T_{1u} + 2T_{2u} + 2G_u + 2H_u \quad (21)$$

$$\Gamma(l=3) = A_g + T_{1g} + T_{2g} + 2G_g + 3H_g + A_u + T_{1u} + T_{2u} + 2G_u + 3H_u \quad (22)$$

$$\Gamma(l=4) = A_g + G_g + 2H_g + T_{1u} + T_{2u} + G_u + H_u \quad (23)$$

$$\Gamma(l=5) = A_g + G_g + H_g \quad (24)$$

$C_{2v}$ , and  $D_{3d}$  of the pairs with different separations. For  $C_{60}$ , the vertex representation is

$$\Gamma_\sigma(60) = A_g + T_{1g} + T_{2g} + 2G_g + 3H_g + 2T_{1u} + 2T_{2u} + 2G_u + 2H_u \quad (25)$$

and

$$[\Gamma_\sigma(60)^2] - \Gamma_\sigma(60) = 23A_g + 37T_{1g} + 37T_{2g} + 60G_g + 83H_g + 14A_u + 44T_{1u} + 44T_{2u} + 58G_u + 72H_u \quad (26)$$

again implying a single orbit of vertices but now 23 distinct orbits of pairs. A pair with unit separation in  $C_{60}$ , for example, could be one of two types: in a single or a double bond of the



main Kekulé structure (pentagon-hexagon or hexagon-hexagon edges, respectively).  $D$  for  $C_{60}$  is 9. The bound (16) is sharp for  $C_{20}$  but not for  $C_{60}$ .

Several properties of the spectrum of the  $\mathbf{D}$  matrix follow easily from its definition. All elements of  $\mathbf{D}$  are integers, and so all moments  $\mu_r = \sum_{i=1}^n (\lambda_i^D)^r$  of the spectrum are also integral.  $\mathbf{D}$  is traceless, and therefore, its eigenvalues sum to zero:

$$\mu_1 = \sum_{i=1}^n \lambda_i^D = 0 \quad (27)$$

Inspection of some sample spectra<sup>5,6</sup> suggests that for fullerenes and other polyhedra there is generally one large positive eigenvalue  $\lambda_1^D \approx 2W/n$ , approximately counterbalanced by three large negative eigenvalues  $\lambda_{n-2}^D \approx \lambda_{n-1}^D \approx \lambda_n^D$ . The remainder of the spectrum is crowded around zero, with a scatter of small positive and negative values, and often, but not invariably, it will include a highly degenerate zero eigenvalue.

The appearance of just one large positive eigenvalue in the spectrum can be rationalized by noting the resemblance between  $\mathbf{D}$  and another familiar off-diagonal matrix. If all nonzero distances in  $\mathbf{D}$  were replaced by their average,  $\bar{d}$ , the new matrix  $\bar{\mathbf{D}}$  would have one eigenvalue  $\bar{D}$  and  $(n-1)\bar{d} = 2W/n$  and  $(n-1)$  eigenvalues  $-\bar{d}$ , as  $\bar{\mathbf{D}}$  would be a scaled version of the adjacency matrix of the complete graph on  $n$  vertices.  $\lambda_1^D$  is a relic of this ancestry. The ground eigenvector of  $\mathbf{D}$  has coefficient  $1/\sqrt{n}$  on every vertex. In the one-orbit case, where all vertices of the graph are equivalent by symmetry, this would also be an eigenvector of  $\mathbf{D}$  with eigenvalue  $\lambda_1^D$  exactly equal to  $2W/n$ , the sum of the unique distance pattern level. The equality holds for, e.g., cycles  $C_n$ , prisms and antiprisms, the platonic and archimedean polyhedra, and the complete graphs  $K_n$ . In the fullerene class, the equality is forced by symmetry for  $C_{20}$  and  $C_{60}$  only but also occasionally holds "accidentally".  $\mathbf{D}$  for  $C_{80}$  has two distinct DLP, but both sum to 440. One  $A_g$  eigenvector has equal contributions on all vertices and  $\lambda = 440$ ; the other has  $\lambda = 0$  and coefficients in the ratio  $-3:1$  on hexagonal:pentagonal vertices. The same two eigenvectors correspond to eigenvalues  $+3$  and  $-1$  of the adjacency matrix of  $C_{80}$ .  $C_{80}$  also therefore obeys (10) exactly, giving  $J = 60/77$ . Likewise, the four-orbit  $C_{240}$  has accidental row-sum degeneracy, with all sums equal to 2312, and hence,  $\lambda = 2312$  and  $J = 8100/17629$ . For multiorbit cases,  $\lambda_1^D \geq 2W/n$ , because the largest eigenvalue of a nonnegative real symmetric matrix is at least the average row sum and the ground eigenvector of  $\mathbf{D}$  has in general a different coefficient for each orbit of vertices.

A more detailed understanding of the spectrum of  $\mathbf{D}$  follows from the spherical model for a polyhedron. In this picture, the 3D structure of the polyhedron is replaced by an average spherical shell onto which all vertices are projected and the  $n$  eigenvectors are then approximated by sampling the first  $n$  independent spherical harmonics at the vertex positions. Models of this kind have been useful in the qualitative theory of electronic, geometrical, and vibrational structure of clusters.<sup>22-26</sup>

In the spherical model, the ground eigenvector of  $\mathbf{D}$  is then the nodeless "S" harmonic (angular momentum  $L = 0$ ), and the three "P" harmonics (angular momentum  $L = 1$ ) account for the trio of large negative eigenvalues noted earlier. Initially, the eigenvalues will be dominated by contributions from antipodal and near-antipodal points and, hence, will tend to take positive signs for the *gerade* harmonics  $L = 0, 2, 4$ , etc. and negative for the *ungerade*  $L = 1, 3, 5$ , etc. As  $L$  rises, the number of angular nodes increases and internal cancellation causes the

spectrum to crowd toward zero. The idealized spherical distance spectrum therefore has a folded pattern

$$S > D > G > \dots > H > F > P \quad (28)$$

with degeneracies  $2L + 1$ . This sequence is in contrast to the model adjacency spectrum, where eigenvalues fall monotonically with  $L$ :

$$S > P > D > F > \dots \quad (29)$$

Point-group induced splittings and details of the construction of the individual graph may split degeneracies and blur the traces of spherical ancestry of the eigenvalues for both  $\mathbf{A}$  and  $\mathbf{D}$ , but the spherical sequence remains a useful guide for symmetrical systems. A more detailed spherical-harmonic theory of distance spectra of polyhedra could be developed along the lines of Stone's tensor-surface harmonic treatment of their adjacency spectra.<sup>22</sup>

Table 2 lists the analytical forms of the distance and adjacency eigenvalues for  $C_{20}$  and  $C_{60}$ , and Figure 2 shows their relation to the spherical classification. The range of the spectrum of  $\mathbf{A}$  is always  $3 \geq \{\lambda^A\} \geq -3$  for a trivalent polyhedron, but the range of the distance spectrum when expressed in units of the largest eigenvalue is predicted to shrink with  $n$  as the sphere is sampled at more points, and indeed, the calculated separation  $(\lambda_1^D - \lambda_n^D)/\lambda_1^D$  does fall from 1.333 for the tetrahedron to 1.274 for the dodecahedron and 1.248 for the truncated icosahedron.

An intriguing aspect of the fullerene distance spectra presented in ref 6 is that whereas nearly all contain zero eigenvalues with high multiplicity (e.g., 9 for  $C_{20}$ , 24 for  $T_d C_{40}$ , 63 for  $I_h C_{80}$ ) some highly symmetric graphs have no zero at all. Some statistics on the distribution of this eigenvalue for wider samples of fullerene and nonfullerene cubic polyhedra are given below.

All of these features of distance spectra can be seen more clearly for monocyclic rings, where a full analytical solution is available. As is well-known from Hückel theory,<sup>27</sup> the eigenvectors and eigenvalues of the adjacency matrix of an  $N$ -gon can be classified by an axial angular momentum quantum number  $\Lambda$  ( $= 0, \pm 1, \pm 2, \dots, \pm(N-1)/2$  ( $N$  odd) or  $\pm N/2$  ( $N$  even)). The eigenvalues are

$$\lambda_\Lambda^A = 2 \cos(2\pi\Lambda/N) \quad (30)$$

and are degenerate for  $\pm|\Lambda|$ ; singly degenerate eigenvalues occur for  $\Lambda = 0$  (all  $N$ ) and  $\Lambda = \pm N/2$  ( $N$  even). The coefficient on vertex  $r$  ( $r = 1, \dots, N$ ) for a vector with eigenvalue  $\Lambda$  can be chosen as

$$c_{r,\Lambda} = (1/\sqrt{N}) \exp(2\pi i(r-1)/N) \quad (31)$$

Because the adjacency eigenvectors for each  $|\Lambda|$  span distinct irreducible representations of the cyclic group,  $C_N$ , they are simultaneous eigenvectors of both  $\mathbf{A}$  and  $\mathbf{D}$ . With some work, the eigenvalues of  $\mathbf{D}$  can therefore be obtained as expectation values over these vectors. All monocycles have a nondegenerate largest distance eigenvalue

$$\Lambda_{\Lambda=0}^D = 2W/N \quad (32)$$

(here  $W = 1/8(N-1)N(N+1)$  for odd  $N$ ,  $1/8N^3$  for even  $N$ ), and the other terms  $\lambda_\Lambda^D$  in the spectrum are  $-1/4 \csc^2(\pi\Lambda/2N)$  ( $N$  odd,  $\Lambda$  odd),  $-1/4 \sec^2(\pi\Lambda/2N)$  ( $N$  odd,  $\Lambda$  even),  $-\csc^2(\pi\Lambda/2N)$  ( $N$  even,  $\Lambda$  odd), and 0 ( $N$  even,  $\Lambda$  even). This last case implies that when  $N$  is even,  $\mathbf{D}$  has a  $(N-2)/2$ -fold degenerate zero eigenvalue.

**TABLE 2: Spectra of Adjacency and Distance Matrices of  $C_{20}$  and  $C_{60}$ , Classified According to Irreducible Representations (irreps) of Icosahedral Point-Group Symmetry<sup>a</sup>**

irrep	$\lambda^A (C_{20})$	$\lambda^D (C_{20})$	$\lambda^A (C_{60})$	$\lambda^D (C_{60})$
$A_g$	+3	+50	+3	+278
$T_{1g}$			$(\sqrt{5} - 3)/2$	$+\phi$
$T_{2g}$			$-\phi^2$	$-\phi^{-1}$
$G_g$	-2	0	+1, -2	$-(2 \pm \sqrt{5})$
$H_g$	+1	0	$+1, (1 \pm \sqrt{13})/2$	-2.9275, 0.8784, 3.0791 <sup>b</sup>
$A_u$				
$T_{1u}$	$+\sqrt{5}$	$-7 - 3\sqrt{5}$	$(\phi^2 \pm \sqrt{9 - \phi^{-1}})/2$	-69.0607, -1.8622 <sup>*c</sup>
$T_{2u}$	$-\sqrt{5}$	$-7 + 3\sqrt{5}$	$(\phi^{-2} \pm \sqrt{9 + \phi})/2$	-5.466, -0.6213 <sup>*c</sup>
$G_u$	0	-2	$-(\sqrt{17} \pm 1)/2$	$-(3 \pm \sqrt{8})$
$H_u$			$\phi^{-1}, -\phi$	$-(3 \pm \sqrt{5})$

<sup>a</sup>  $\{\lambda^A\}$  are eigenvalues of the adjacency matrix  $\mathbf{A}$ ,  $\{\lambda^D\}$  are the eigenvalues of the distance matrix  $\mathbf{D}$ . <sup>b</sup> Solutions of  $\lambda^3 - \lambda^2 - 9\lambda + 8$ . <sup>c</sup>  $T_{1u}$  and  $T_{2u}$  solutions together are the roots of  $\lambda^4 + 77\lambda^3 + 563\lambda^2 + 1022\lambda + 436$ .

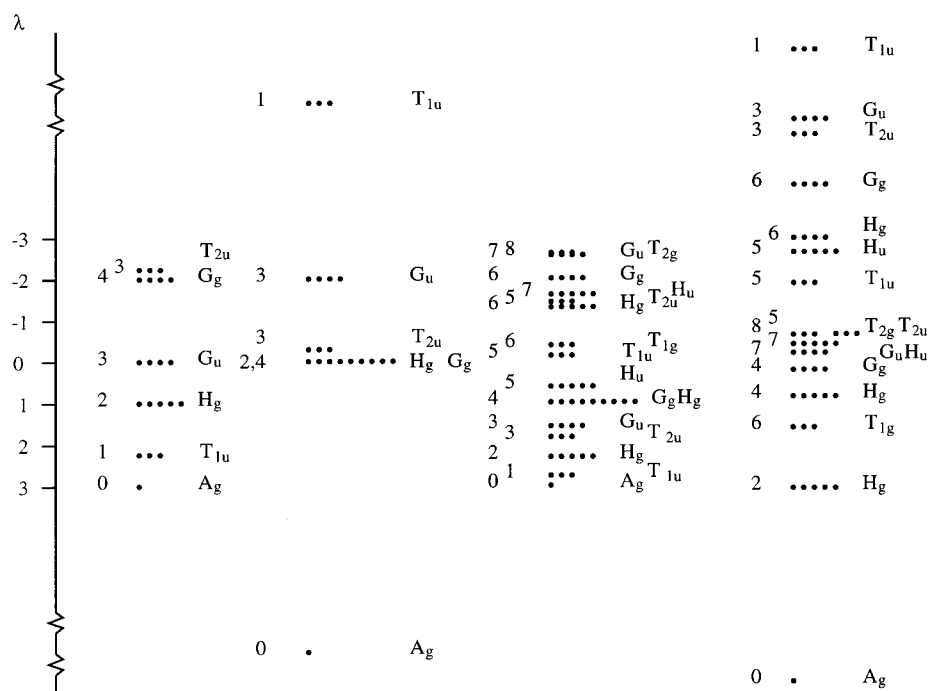


**Figure 2.** Spherical harmonic interpretation of adjacency and distance eigenvalue spectra of fullerenes. Spectra of the adjacency (left) and distance matrix (right) of (a)  $C_{20}$  and (b)  $C_{60}$  are labeled by irreducible representations within  $I_h$  symmetry ( $A_g, T_{1g}, \dots$ ) and angular momentum within the spherical group ( $L = 0, 1, 2, \dots$ ). Adjacency spectra are roughly monotonic in  $L$ , but distance spectra converge on the zero eigenvalue from opposite directions for odd and even values of  $L$ .

This simple monocyclic problem exhibits the relation of the largest eigenvalue to the Wiener index, the folding of the  $\Lambda$  series about zero,

$$\Lambda_{\Lambda=0}^D > \Lambda_{\Lambda=2}^D > \dots > \Lambda_{\Lambda=3}^D > \Lambda_{\Lambda=1}^D \quad (33)$$

the multiple zero eigenvalues seen for some systems, and systematic absence of zeros for others, all as observed for fullerene polyhedra.

## 5. Algorithms

Calculation of distance matrices is a standard operation in computational graph theory and highly efficient procedures are known. The simplest algorithm for unweighted sparse graphs consists of finding distances from each vertex in turn, chosen as origin for shortest paths to all others. To do this, the chosen vertex is labeled 0, unlabeled neighbors receive the label 1, their unlabeled neighbors receive label 2, etc. This algorithm is easy to use by hand, even for fairly large graphs, and very quick on

a computer. For each vertex, the number of operations is proportional to the number of edges. (One must check once for all edges incident with a given vertex whether their neighbors are unlabeled and, if so, label and store them.) Because the edge count is  $O(n)$  for chemical graphs, which have a bounded vertex degree, and equal to  $3n/2$  for cubic graphs, the total number of operations is  $O(n^2)$ . Because the distance matrix which is the output has  $n^2$  elements, there is a lower bound of  $\Omega(n^2)$  on the number of operations and the algorithm is the best possible, up to a constant factor, i.e., it is  $\theta(n^2)$ .

Contrast this  $\theta(n^2)$  algorithm with the procedure based on taking powers of the adjacency matrix.<sup>5,6</sup>  $\mathbf{A}$  contains information of walks of unit length and, in general, the element  $(\mathbf{A}^N)_{ij}$  of its  $N$ th power is equal to the number of walks of length  $N$  that go from vertex  $i$  to  $j$ . A strategy for computing  $\mathbf{D}$  is therefore to take successively higher powers, setting each  $D_{ij}$  to the lowest value of  $N$  for which  $(\mathbf{A}^N)_{ij}$  is nonzero. The matrix multiplication is carried on until every element has been set, i.e., until the cumulative total  $\mathbf{1} + \mathbf{A} + \mathbf{A}^2 + \mathbf{A}^3 + \dots$  no longer has zero entries. This algorithm is conceptually straightforward, but its

**TABLE 3: Distance Invariants of Icosahedral Fullerenes  $C_n$  with  $n \leq 3000^a$** 

$n$	$i$	$j$	$R$	$D$	$W$	$S_z$	$J$	$i_z$	$\lambda_{\max}^D$
20	1	0	5	5	500	1920	1.50000	9	50
60	1	1	9	9	8340	51840	0.91052	0	278
80	2	0	11	11	17600	157440	0.77922	63	440
140	2	1	13	14	71390	753390	0.60058	24	1019.87
180	3	0	15	17	135120	1890780	0.52790	127	1501.68
240	2	2	19	19	277440	4250880	0.45947	170	2312
260	3	1	19	19	338800	5357580	0.44215	0	2606.25
320	4	0	21	23	571620	10931100	0.39819	222	3573.59
380	3	2	23	24	878040	17203020	0.36618	68	4621.28
420	4	1	24	25	1127970	23888730	0.34858	0	5371.71
500	5	0	25	29	1747500	42383040	0.31942	366	6992.00
540	3	3	27	29	2119320	51606900	0.30731	370	7849.56
560	4	2	28	28	2319730	57064260	0.30202	157	8284.80
620	5	1	29	31	2991650	79177380	0.28729	50	9651.68
720	6	0	31	35	4352340	127954500	0.26659	461	12093.39
740	4	3	32	34	4663630	133992780	0.26278	60	12604.59
780	5	2	33	34	5317320	157738920	0.25613	0	13634.46
860	6	1	33	37	6785730	215120400	0.24414	120	15783.30
960	4	4	37	39	8949420	298962900	0.23075	661	18645.32
980	5	3	37	38	9419270	316200480	0.22848	0	19223.09
980	7	0	35	41	9412420	325192080	0.22871	665	19214.74
1040	6	2	38	39	10922430	381125340	0.22196	140	21005.60
1140	7	1	39	43	13736130	506946960	0.21217	320	24103.02
1220	5	4	41	44	16300010	616623300	0.20479	240	26721.96
1260	6	3	42	43	17663490	681998550	0.20159	562	28037.56
1280	8	0	41	47	18357700	728828460	0.20024	839	28692.51
1340	7	2	43	45	20589850	825868140	0.19565	24	30733.22
1460	8	1	43	49	25506370	1073740980	0.18756	160	34947.58
1500	5	5	45	49	27337500	1160781120	0.18470	1101	36451.50
1520	6	4	46	48	28251090	1205984700	0.18353	332	37172.82
1580	7	3	47	48	31109310	1357249230	0.18010	0	39379.62
1620	9	0	45	53	33089280	1484362140	0.17807	1083	40863.27
1680	8	2	48	51	36246150	1643201340	0.17480	130	43154.18
1820	9	1	49	55	44264770	2092969800	0.16804	180	48653.63
1820	6	5	50	54	44339550	2080153920	0.16772	180	48726.23
1860	7	4	51	52	46805160	2226859770	0.16595	40	50328.48
1940	8	3	52	54	51976100	2535951630	0.16259	240	53585.27
2000	10	0	51	59	56046920	2803357200	0.16031	1298	56063.85
2060	9	2	52	57	60355910	60355910	0.15791	160	58604.76
2160	6	6	55	59	68059260	3506532300	0.15396	1392	63020.55
2180	7	5	55	58	69634180	3606283770	0.15328	300	63885.48
2220	10	1	54	61	72751770	3816780120	0.15218	280	65557.83
2240	8	4	56	58	74504060	3910333140	0.15126	887	66522.23
2340	9	3	57	59	83054190	4481563710	0.14809	50	70989.76
2420	11	0	55	65	90275900	4981183440	0.14576	1622	74630.77
2480	10	2	57	63	95989710	5348608500	0.14395	160	77421.66
2540	7	6	59	64	102066310	5715039960	0.14200	300	80369.90
2580	8	5	60	62	106114470	6014477610	0.14092	280	82259.90
2660	11	1	59	67	114347030	6591011400	0.13905	240	85996.66
2660	9	4	61	63	114491360	6596544960	0.13884	0	86085.22
2780	10	3	62	65	127773510	7556572200	0.13590	60	91929.13
2880	12	0	61	71	139494600	8416987680	0.13364	1837	96900.62
2940	11	2	62	69	146891400	8944767630	0.13224	520	99941.66
2940	7	7	63	69	147148500	8914967280	0.13199	2012	100105.45
2960	8	6	64	68	149645420	9109938660	0.13156	390	101113.72

<sup>a</sup> Each fullerene is labeled by the two Goldberg parameters<sup>28</sup>  $i, j$ , that specify its net.  $R$  and  $D$  are the radius and diameter of the graph.  $W, S_z$ , and  $J$  are its Wiener, Szeged, and Balaban indices, respectively. The distance spectrum has  $i_z$  zero eigenvalues and largest positive eigenvalue  $\lambda_{\max}^D$ .

complexity is  $O(n^4)$  and it rapidly becomes unworkable when large graphs or large numbers of graphs are to be considered.

The relative efficiency of the first algorithm is illustrated by Table 3, where  $R, D, W, J$ , distance level patterns, largest eigenvalues, and numbers of zeroes in the distance spectrum are listed for all icosahedral fullerenes  $C_n$  on  $n \leq 3000$  vertices. The fullerenes are generated by the Goldberg construction.<sup>28</sup> Calculations of  $R, D, W, S_z, J$ , and DLP take a few seconds in total; it is estimated that the second algorithm would take orders of magnitude longer to produce these data. Given that each icosahedral fullerene is constructible using just two integers,<sup>28</sup>

it is tempting to speculate that the invariants in Table 3 should all be analytical functions of the Goldberg parameters. At least as far as the tabulation is taken, diameters of the  $I_h$  fullerenes fit the formulas  $D(i,i) = 6i - 1$  and  $D(i,0) = 10i - 1$ , and the radii fit  $R(i,i) = 9i + 1 - i \pmod{2}$  and  $R(i,0) = 5i + 1 - i \pmod{2}$ . Relations for other invariants and for the chiral cases appear to be more complicated.

Hints of other regularities are also evident in the table. The relationship (10) between  $W$  and  $J$ , which was derived only for the case when all rows of the distance matrix have the same sum, is in fact obeyed surprisingly closely by all of the icosahedral fullerenes tested. For four members of the series ( $C_{20}$ ,  $C_{60}$ ,  $C_{80}$ , and  $C_{240}$ ), the relationship is exact, in the first two cases because the row sums are equal by symmetry and in the others because the sums are equal by accident, as noted earlier. In all other cases in the Table, the fullerene has more than one row sum but the quotient  $4(v+4)W/J/9n^3$  exceeds unity by less than  $3 \times 10^{-4}$ .

## 6. Results

Given an efficient algorithm, it is possible to make a systematic examination of the chemical relevance of Wiener and related indices for fullerenes. Calculations were performed on three test sets: (i) complete sets of cubic polyhedra  $P_n$  on  $n$  vertices ( $n = 20, 22$ , and  $24$ ), (ii) the complete set of fullerenes  $C_n$  on 60 vertices, and (iii) complete sets of isolated-pentagon fullerenes  $C_n$  ( $n = 84$ , and  $100$ ). Set i was generated using the "plantri" program of Brinkmann and McKay;<sup>29</sup> sets ii and iii, from the spiral algorithm of Manolopoulos et al.<sup>30</sup> More efficient procedures for fullerene generation are known,<sup>31</sup> but the spiral encodes symmetry and other properties of the graphs in a transparent way<sup>32</sup> and forms part of standard IUPAC nomenclature for the molecules.<sup>33</sup> The strategy with each set is to compare the performance of the distance invariants with in each case an invariant that is already known to correlate with total energy.

(i) **Cubic Polyhedra.** Within the combinatorially explosive number of all cubic (trivalent) polyhedra, fullerenes form a tiny subset. Chemically, however, they are favored structures for carbon cages, and their special role is confirmed by explicit computation of relative energies. A simple measure of proximity of a given cubic polyhedron to a fullerene is the  $F$  parameter<sup>34</sup>

$$F = \sum_r f_r (6-r)^2 \quad (34)$$

where  $f_r$  is the number of faces of size  $r$ . If a fullerene exists for the given number of vertices, it will have  $F = 12$  ( $f_5 = 12$  and  $f_6 = n/2 - 10$ ), and this is the minimum possible. Where a fullerene does not exist, ( $n < 20$  and  $n = 22$ ), the polyhedron of minimal  $F$  is still apparently that of lowest energy.<sup>34</sup>  $F$  can therefore be used to rank cubic polyhedra, at least crudely, for relative energy.

Figure 3 shows scatter diagrams for the Wiener index  $W$  and  $J$  against  $F$  for 20-, 22- and 24-vertex cubic polyhedra. All three indices are highly degenerate,<sup>7</sup> as is  $F$  itself, and the plotted distributions show wide dispersion. However,  $W$  and  $J$  show good selectivity for fullerenes. The two  $F = 12$  data points for the unique fullerenes  $C_{20}$  and  $C_{24}$  (marked by crosses) stand out from the cloud of  $(F, W)$  and  $(F, J)$  pairs. For  $C_{22}$ , the situation is less clear, as the minimum- $W$ /maximum- $J$  points have  $F = 16$ , beating narrowly the near-fullerene at  $F = 14$  ( $f_4 = 1, f_5 = 10$ , and  $f_6 = 2$ ). The differences in  $W$  (645 vs 646) and  $J$  (1.414 35 vs 1.426 98) are small, and this is compatible

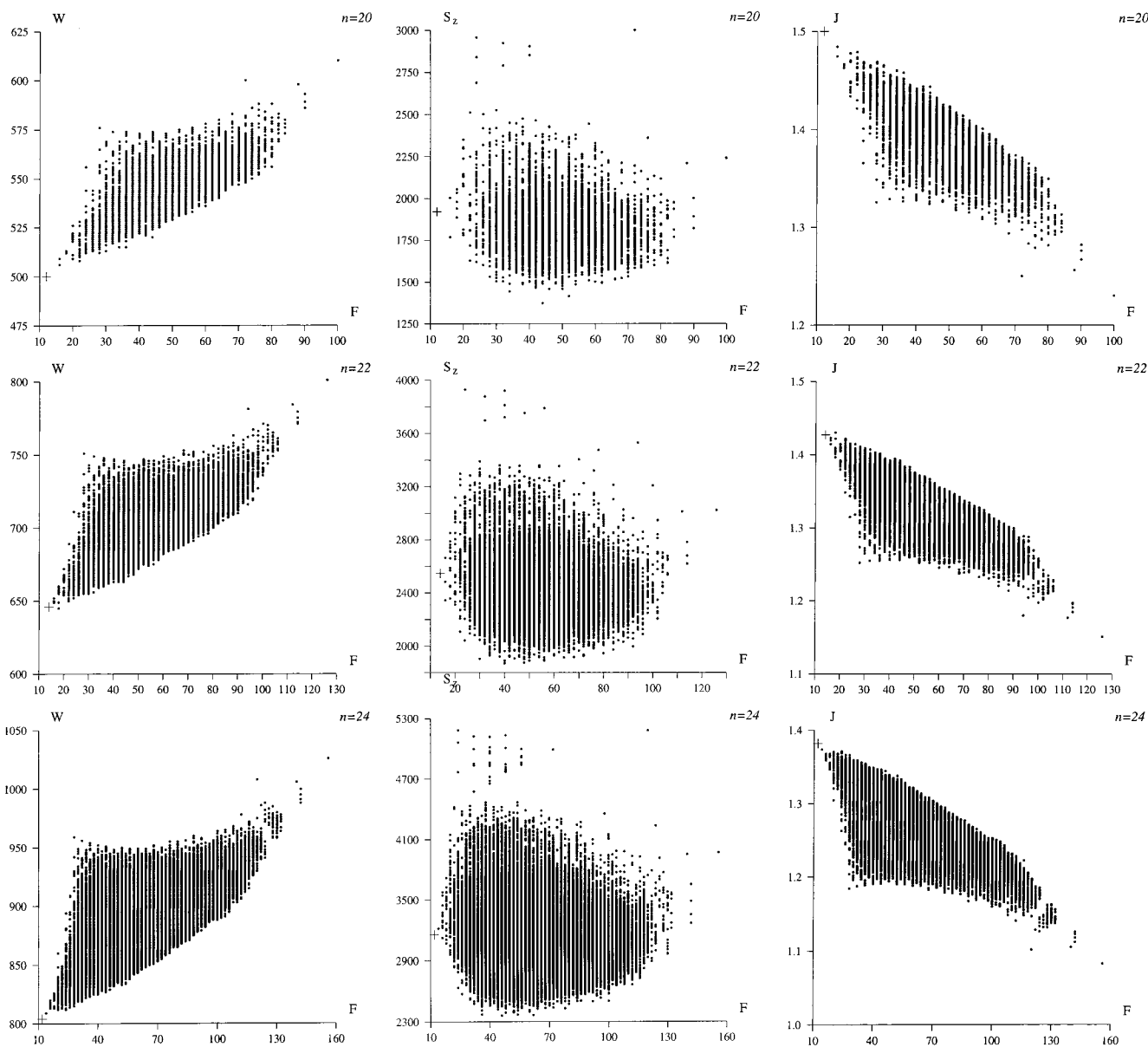


**Figure 3.** Distance invariants for general cubic polyhedra. (a) Wiener index,  $W$ , (b) Szeged index,  $S_z$ , (c) Balaban index,  $J$ , for the complete sets<sup>29</sup> of (top to bottom) 7595 20-, 49 566 22-, 339 722 24-vertex cubic polyhedra, plotted against  $F$ , (34), which measures the deviation of each polyhedron from the fullerene ideal ( $F = 12$ ). The unique fullerenes  $C_{20}$  and  $C_{24}$  and the minimal- $F$   $C_{22}$ <sup>34</sup> are shown as crosses on the diagrams.

with the small difference in computed energy of the carbon cages.<sup>34</sup> In contrast, the Szeged index shows no preference for the fullerenes and near-fullerenes; the minimal- $F$  cages lie in the middle of the range and would not be picked out without other information. Thus, only two of the three indices are able to pick out the fullerene or near-fullerene cages from the mass of general cubic polyhedra. This feature is of course shared by the easily computed  $F$  function.

Wiener and Balaban indices can be expected to be closely related, because both depend on the row sums of the distance matrix and, as we have seen, they give the same predictions for extremal polyhedra. In addition, Figure 4 shows that  $W$  and  $J$  also follow closely an inverse proportionality relation for nonextremal polyhedra. The whole set of 7595 20-vertex polyhedra cluster around the hyperbola predicted by (10) for fully symmetric polyhedra. Though not as close a fit as noted earlier for the icosahedral fullerenes, this is a clear indication that the two invariants share the same physical content.

**(ii) General Fullerenes.** It is known that a major determinant of energy of small fullerenes is the number of pentagon

adjacencies.<sup>35,36</sup> Each pentagon fusion in a fullerene cage carries an energy penalty of the order of 1 eV, and the isomers of lowest energy at each  $n$  have the lowest achievable number,  $N_p$ , of such fusions. Pentagon adjacencies are forced for all  $n < 60$ .

Figure 5 shows scatter diagrams for the Wiener index  $W$ ,  $S_z$ , and  $J$  against the number of pentagon adjacencies for the fullerene isomers of  $C_{60}$ . It is clear that  $W$ ,  $S_z$ , and  $J$  have a qualitative tendency to select fullerenes of low  $N_p$  and, hence, pick out the class of low-energy isomers. The unique isolated-pentagon  $C_{60}$  cage minimizes  $W$  and  $S_z$  and maximizes  $J$  within the set. The broad scatter for  $S_z$  vs  $N_p$  again suggests that the Szeged index is less physically relevant than  $W$  or  $J$ . The stronger correlation for  $W$  and  $J$  is again a useful feature, though it does not improve on the known and easily calculated  $N_p$ . The degeneracy of  $W$  as an index for the  $C_{60}$  fullerenes was noted by Balaban et al.;<sup>7</sup> the 1812 isomers support only 116 distinct values of  $W$  which, according to the criterion used in ref 7, indicates an information deficit of 5.1062 for this index. Our interest here is somewhat different, in that, the aim is not to find an index that distinguishes all isomers but one that picks



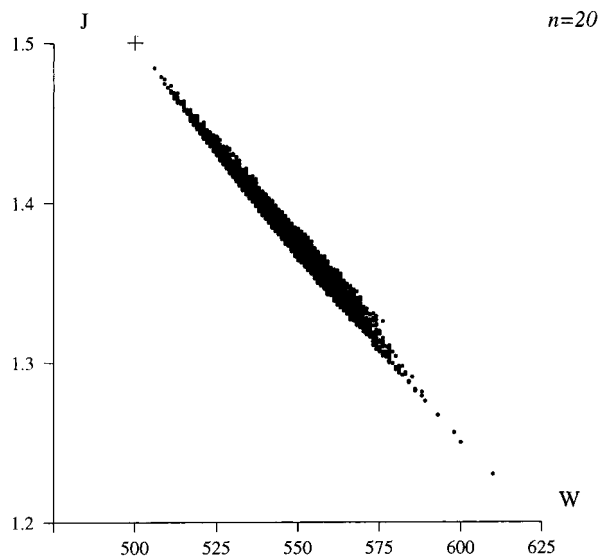


**Figure 4.** Correlation between  $W$  and  $J$  indices for the 20-vertex polyhedra. The curve for fully symmetric polyhedra in which all 20 vertices are equivalent ( $WJ = 750, (10)$ ) is closely followed, even though only  $I_h C_{20}$  satisfies this requirement rigorously.

out low-energy structures from general fullerenes; in this respect,  $W$ ,  $S_z$ , and  $J$  are all successful.

**(iii) Isolated-Pentagon Fullerenes.** Beyond the very clear indications of the isolated-pentagon (minimal pentagon adjacency) rule, it is less easy to predict the fine detail of the energy ordering among the class of favored isomers. Some progress can be made with the hexagon-neighbor index  $H$  which, for example, rationalizes the predictions of a number of independent quantum mechanical methods that isomers 84:22 and 84:23 (in the spiral notation) are the iso-energetic best of the set of 24  $C_{84}$  fullerenes,<sup>37</sup> a result in agreement with experimental isomer ratios<sup>38</sup> and selects low-energy candidates from 6063 isolated-pentagon isomers of  $C_{116}$ .<sup>39</sup>  $H$  can be defined as the second moment property<sup>32</sup>

$$H = \sum_k k^2 h_k \quad (35)$$

where  $h_k$  is the number of hexagonal faces of a fullerene which have exactly  $k$  hexagonal neighbors.

Correlation with distance invariants is poor within this tightly defined set. For example, the 24 isolated-pentagon isomers of  $C_{84}$  (Table 4) span a range in  $H$  from 548 to 572, with three isomers (84:21, 84:22, and 84:23) achieving the minimal value, of which two are iso-energetic components of the experimental product.<sup>38</sup> Minimization of  $W$ , or maximization of  $J$ , would select the least stable of the IPR isomers, 84:1, and minimization of  $S_z$  would select 84:4, also energetically unfavorable. Clearly, a pure strategy of finding extremal distance invariants does not yield the low-energy isomers. The next example,  $C_{100}$ , gives the clue to a more successful strategy. Plots of  $W$ ,  $S_z$ , and  $J$  vs  $H$  show (Figure 6) that the isomer favored in quantum-mechanical energy calculations,<sup>40</sup> ( $D_2 100:459$ ) which is an expansion of the experimental  $C_{76}$  isomer, is one of 38 with the minimal value of  $H$  (820), but for that value of  $H$ , it is the isomer with the lowest  $W$  and  $S_z$  and highest  $J$ . Thus, although  $W$ ,  $S_z$ , or  $J$  alone cannot select the low-energy isomer from the already favored isolated-pentagon set, any one of the pairings ( $H,W$ ), ( $H,S_z$ ), or ( $H,J$ ) suffices to pick the known best isomer out of the 450 candidates.

An optimum strategy for finding low-energy carbon cages would seem to be to first minimize  $F$  to find the fullerene

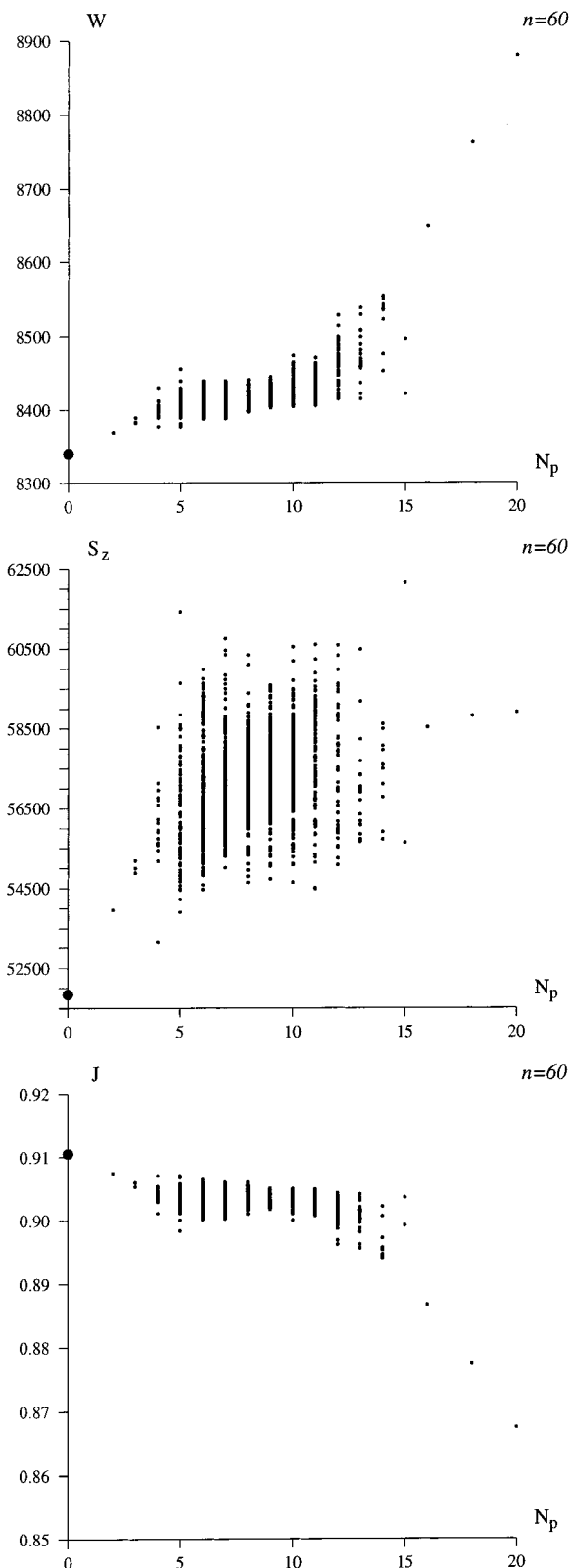


**Figure 5.** Distance invariants for 1812 fullerene isomers<sup>32</sup> of  $C_{60}$ . (a) Wiener index,  $W$ , (b) Szeged index,  $S_z$ , (c) Balaban index,  $J$ , (top to bottom), plotted against  $N_p$ , the number of pentagon fusions. The unique isolated-pentagon isomer, corresponding to the experimentally observed  $C_{60}$  molecule, is shown as a large dot in the diagrams.

subclass of cubic polyhedra, then minimize  $N_p$  to find isolated-pentagon fullerenes, then minimize  $H$ , and finally minimize  $W$  or  $S_z$ .

**(iv) Distance Spectra.** As the spherical harmonic model of the distance spectrum shows, the largest eigenvalue of  $\mathbf{D}$  carries

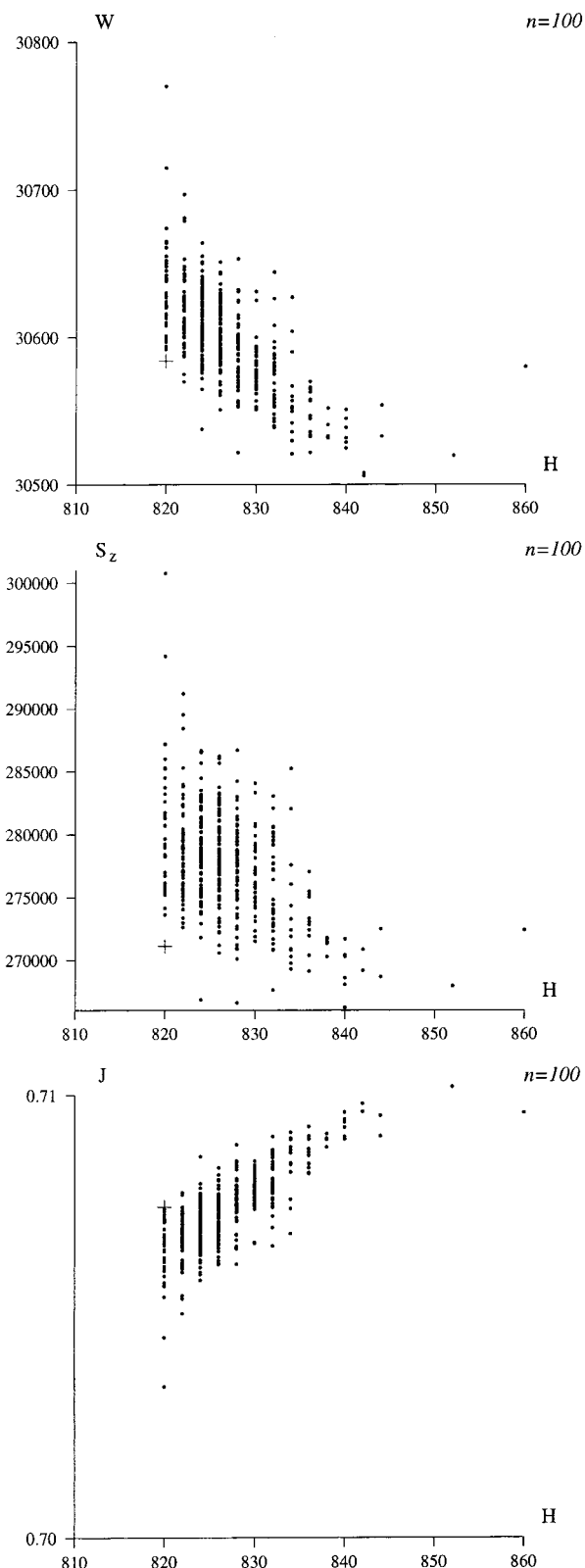


**Figure 6.** Distance invariants for 450 isolated-pentagon fullerene isomers<sup>32</sup> of  $C_{100}$ . (a) Wiener index,  $W$ , (b) Szeged index,  $S_z$ , (c) Balaban index,  $J$ , (top to bottom), plotted against  $H$ , the hexagon neighbor signature second moment. The cross marks 100:449, the isomer predicted to be of lowest total energy.<sup>40</sup>

information similar to that from the Wiener index itself. The variation in the number of zero eigenvalues is potentially more discriminating. Of the 7595 20-vertex trivalent polyhedra, the numbers of isomers  $N(i_z)$  with  $i_z$  zeros are 4770(0), 1636(1), 719(2), 250(3), 112(4), 54(5), 22(6), 10(7), 13(8), 3(9), 1(10),

**TABLE 4: Invariants for the 24 Isolated-Pentagon Isomers<sup>32</sup> of  $C_{84}$ <sup>a</sup>**

$n:m$	$G$	$R$	$D$	$W$	$S_z$	$J$	$H$
84:1	$D_2$	10	11	19646	156660	0.77197	572
84:2	$C_2$	10	11	19664	156576	0.77114	564
84:3	$C_s$	10	11	19686	157409	0.76997	554
84:4	$D_{2d}$	10	11	19666	155138	0.77088	556
84:5	$D_2$	10	11	19682	156280	0.77032	556
84:6	$C_{2v}$	10	11	19674	157602	0.77036	556
84:7	$C_{2v}$	10	11	19712	160766	0.76887	552
84:8	$C_2$	10	11	19699	159246	0.76939	552
84:9	$C_2$	10	11	19715	161714	0.76875	552
84:10	$C_s$	10	11	19730	163094	0.76814	550
84:11	$C_2$	10	11	19705	161662	0.76910	552
84:12	$C_1$	10	11	19723	162869	0.76840	550
84:13	$C_2$	10	11	19730	163964	0.76813	552
84:14	$C_s$	10	11	19688	159972	0.76979	556
84:15	$C_s$	10	11	19714	161336	0.76875	550
84:16	$C_s$	10	11	19714	163298	0.76874	552
84:17	$C_{2v}$	10	11	19724	164344	0.76837	554
84:18	$C_{2v}$	10	11	19704	162692	0.76914	556
84:19	$D_{3d}$	11	11	19716	163848	0.76867	552
84:20	$T_d$	10	11	19686	162054	0.76987	564
84:21	$D_2$	10	11	19734	163248	0.76796	548
84:22	$D_2$	10	11	19720	162756	0.76849	548
84:23	$D_{2d}$	10	11	19718	162182	0.76857	548
84:24	$D_{6h}$	11	11	19716	163896	0.76866	552

<sup>a</sup>  $G$  is the maximum symmetry of the polyhedron,  $H$  is the second moment of the hexagon neighbor signature (35), and  $W$ ,  $S_z$ , and  $J$  are the Wiener, Szeged, and Balaban indices.

4(11), and 1(13). The polyhedron of highest symmetry, the dodecahedron, has a high but not maximal number of zeros (9); the unique polyhedron with 13 zeros is the dodecagonal prism. The 1812  $C_{60}$  fullerenes again exhibit a descending series for  $N(i_z)$  [741(0), 406(1), 258(2), 120(3), 84(4), 45(5), 39(6), 40(7), 29(8), 17(9), 5(10), 9(11), 4(12), 3(13), 3(14), 3(15), 3(16), 1(20), 1(23), and 1(26)], but now the most symmetrical and unique isolated-pentagon fullerene is just one of many without a zero eigenvalue. The extremal 26-zero case is the cylinder with hemidodecahedral caps. For the icosahedral fullerenes listed in Table 3, the number of zero distance eigenvalues varies erratically with the number of vertices. At 980 vertices, for example, one icosahedral fullerene has 665 zeros and the other has none. Some systematics undoubtedly lie behind these numbers, but  $i_z$  does not appear to be directly related to isomer energy.

## Conclusion

Distance matrices give rise to a variety of connected invariants—the radius; diameter; set of distance level patterns; distance eigenvalues; Hosoya polynomials; Wiener, Szeged, and Balaban indices; and many others. The simplest distance invariants can be computed cheaply for fullerenes and other polyhedra. They offer discrimination between fullerenes and nonfullerenes and between isolated-pentagon and general fullerenes. In combination with hexagon-neighbor information, they have been shown to select low-energy isomers from among the isolated-pentagon fullerenes at  $C_{84}$  and  $C_{100}$ . More detailed consideration of the distance level patterns or distance spectra may offer further insight; the present paper has corrected literature statements on the former and given the basis for a qualitative interpretation of the latter in terms of spherical harmonics.

## References and Notes

- (1) Wiener, H. *J. Am. Chem. Soc.* **1947**, *69*, 17; 2636.
- (2) Klein, D. J.; Zhu, H.-Y. *J. Math. Chem.* **1998**, *23*, 179.

- (3) See, for example, the special issue of *MATCH* for the 50th birthday of the Wiener Index **1997**, 35, 259; Gutman, I., Klavžar, S., Mohar, B., Eds.
- (4) Ori, O.; Marenzoni, P. *Mol. Simulation*, **1993**, 11, 365.
- (5) Balasubramanian, K. *Chem. Phys. Lett.* **1995**, 239, 117.
- (6) Balasubramanian, K. *J. Phys. Chem.* **1995**, 99, 10785.
- (7) Balaban, A. T.; Liu, X.; Klein, D. J.; Babic, D.; Schmalz, T. G.; Seitz, W. A.; Randić, M. *J. Chem. Inf. Comput. Sci.* **1995**, 35, 396.
- (8) Gutman, I. *Graph Theory Notes New York* **1994**, 27, 9.
- (9) Gutman, I.; Popović, L.; Khadikar, P. V.; Karmarkar, S.; Joshi, S.; Mandloi, M. *MATCH*, **1997**, 35, 91.
- (10) Balaban, A. T. *Chem. Phys. Lett.* **1982**, 80, 399.
- (11) Randić, M. *J. Am. Chem. Soc.* **1975**, 97, 6609.
- (12) Fajtlowicz, S. *Discrete Math.* **1988**, 72, 113.
- (13) Fajtlowicz, S. *Written On The Wall: A list of conjectures made by the Graffiti program*. The updated list is available at <http://www.math.uh.edu/~clarson>.
- (14) Fowler, P. W.; Rogers, K. M.; Fajtlowicz, S.; Hansen, P.; Caporossi, G. Facts and conjectures about fullerene graphs: leapfrog, cylindrical and Ramanujan fullerenes, In *Algebraic Combinatorics and Applications*; Betten, A., Kohnert, A., Laue, R., Wassermann, A., Eds.; Springer Verlag: Berlin, Germany, 2001.
- (15) Balaban, A. T.; Mills, D.; Ivanciuc, O.; Basak, S. *Croat. Chem. Acta* **2000**, 73, 923.
- (16) Asratian, A. S.; Denley, T. M. J.; Häggkvist, R. *Bipartite graphs and their applications, Cambridge Tracts in Mathematics 131*; Cambridge University Press: Cambridge, U.K., 1998.
- (17) Fuji, Z.; Huaian, L. *MATCH* **1997**, 35, 213.
- (18) Hosoya, H. *Discuss. Appl. Math.* **1988**, 19, 239.
- (19) Streitwieser, A., Jr. *Molecular orbital theory for organic chemists*, Wiley: New York, 1961.
- (20) Rouvray, D. H. Characterisation of molecular branching using topological indices. In *Applications of Discrete Mathematics*; Ringeisen, R. D., Roberts, F. S., Eds.; SIAM: Philadelphia, PA, 1988; pp 176–188.
- (21) Chung, F. R. K. *Spectral Graph theory*, CBMS Regional Conference Series in Mathematics 92; AMS: Providence, RI, 1997; pp 118–121.
- (22) Stone, A. J. *Mol. Phys.* **1980**, 41, 1339; Stone, A. J. *Inorg. Chem.* **1981**, 20, 563.
- (23) Mingos, D. M. P.; Wales, D. J. *Introduction to cluster chemistry*; Prentice Hall International: London, 1990.
- (24) Fowler, P. W.; Woolrich, J. *Chem. Phys. Lett.* **1986**, 127, 77.
- (25) Manolopoulos, D. E.; Fowler, P. W. *J. Chem. Phys.* **1992**, 96, 7603.
- (26) Ceulemans, A.; Titeca, B. C.; Chibotaru, L. F.; Vos, I.; Fowler, P. W. Complete force fields for trivalent and deltahedral cages: group theory and applications to cubane, closo-dodecahedrane and buckminsterfullerene. To be published
- (27) See, e.g., Albright, T. A.; Burdett, J. K.; Whangbo, M.-H. *Orbital interactions on Chemistry*; Wiley: New York, 1985; Chapter 12.2.
- (28) Goldberg, M. *Tohoku Math. J.* **1937**, 43, 104.
- (29) Brinkmann, G.; McKay, B. Version 1.0 of the programme *plantri.c* and its documentation are obtainable at <http://cs.anu.edu.au/people/bdm>.
- (30) Manolopoulos, D. E.; May, J. C.; Down, S. E. *Chem. Phys. Lett.* **1991**, 181, 105.
- (31) Brinkmann, G.; Dress, A. W. M. *Adv. Appl. Math.* **1998**, 21, 473.
- (32) Fowler, P. W.; Manolopoulos, D. E. *An atlas of fullerenes*; Oxford University Press: New York, 1995; Vol. VIII, pp 392.
- (33) Godly, E. W.; Taylor, R. *Fullerene Sci. Technol.* **1997**, 5, 1667.
- (34) Domene, M. C.; Fowler, P. W.; Mitchell, D.; Seifert, G.; Zerbetto, F. *J. Phys. Chem. A* **1997**, 101, 8339.
- (35) Campbell, E. E. B.; Fowler, P. W.; Mitchell, D.; Zerbetto, F. *Chem. Phys. Lett.* **1996**, 250, 544.
- (36) Albertazzi, E.; Domene, C.; Fowler, P. W.; Heine, T.; Seifert, G.; Van Alsenoy, C.; Zerbetto, F. *Phys. Chem. Chem. Phys.* **1999**, 1, 2913.
- (37) Raghavachari, K. *Chem. Phys. Lett.* **1992**, 190, 397.
- (38) Manolopoulos, D. E.; Fowler, P. W.; Taylor, R.; Kroto, H. W.; Walton, D. R. M. *J. Chem. Soc., Faraday Trans.* **1992**, 88, 3117.
- (39) Achiba, A.; Fowler, P. W.; Mitchell, D.; Zerbetto, F. *J. Phys. Chem. A* **1998**, 102, 6835.
- (40) Austin, S. J. Systematics of carbon cages, Ph.D. Thesis, University of Exeter, 1995.